Shape matters

Influence of varying settlement profiles due to multicausal subsidence when modelling damage in a masonry façade

Prosperi, Alfonso; Longo, Michele; Korswagen, Paul A.; Korff, Mandy; Rots, Jan G.

Shape matters: Influence of varying settlement profiles due to multicausal subsidence when modelling damage in a masonry façade

Alfonso Prosperi[1], Michele Longo[1], Paul A. Korswagen[1], Mandy Korff[1,2], Jan G. Rots[1]

1 Delft University of Technology, Faculty of Civil Engineering and Geosciences, Stevinweg 1, 2628
2 Deltares, P.O BOX, 177, 2600 MH Delft, The Netherlands
Contact: a.prosperi@tudelft.nl

Abstract

This paper demonstrates the use of non-linear finite element modelling to investigate the response of structures subjected to different shapes of subsidence-related ground settlements. The approach is presented with reference to a two-storey unreinforced masonry façade resting on a shallow foundation. Eight realistic settlement shapes, based on field and literature data, are applied in the model with increasing intensity. The intensity of the subsidence profiles is characterized using their (angular) distortion. The extent of the induced damage on the façade is objectively and directly quantified by a damage parameter, based on the number of cracks, their length and opening. The performance of different settlement indicators and corresponding limiting values, typically employed in the state of the art, is in this paper discussed in relation to the damage modelling strategy; these are observed to be dependent on the shape of the settlement profiles. The aim of this paper is thus to provide insight into the extent to which the vulnerability of masonry buildings depends on the shape of the subsidence pattern and may serve as a warning not to use (deterministic) damage indicators such as angular distortion without considering the settlement shape.

Introduction

When a structure is unable to accommodate the subsidence, cracking of structural or non-structural elements alike, tilting and distortions are likely to occur, leading to a loss of cosmetic, functional or structural aspects (Drougkas et al., 2020, Charles and Skinner, 2004, Burland et al., 1978). When dealing with certain causes of subsidence, such as tunnelling or mining, existing approaches allow estimating both the vertical and horizontal green-field ground movements (i.e., the displacement on the ground surface level if the building were not present) with good accuracy (Drougkas et al., 2020). However, different drivers lead to unpredictable settlement shapes which also depend on the high variability of the buildings' features, their foundation systems and, in turn, the loads transmitted to the inhomogeneous subsurface on which they rest. Therefore, challenges arise in the definition of limiting values for the ground deformations and/or the building's distortions. Several proxy parameters are suggested in the literature and are employed in damage assessment analyses.

For instance, Eurocode 7 (CEN, 2004) suggests that a value of angular distortion (i.e., the slope of two points in relation to the rigid rotation of the structure) of 1/500 (or 2‰) is acceptable for many structures to prevent the occurrence of serviceability damage. However, it may be challenging to confirm the general validity of such values, since data of real full-scale structures are often unavailable or limited. Numerical analyses provide a reliable alternative to investigate the behaviour of masonry façades subjected to ground settlements. The numerical approach herein proposed for a masonry façade on a shallow strip foundation, is used to perform a wide number of analyses, to further investigate the role of different building and soil conditions, while directly and objectively quantifying the damage in terms of cracks on the building.

Description of the finite element modelling approach

In this study, a 2D structural model of a masonry façade, typical of Dutch low-rise residential buildings, is built with the software Diana FEA 10.5, with a height of 7 meters a length of 8 meters (Figure 1), and a thickness of 100 mm. The model is characterized by openings underneath masonry lintels, asymmetrically distributed with respect to a central axis along the length of the façade. The opening ratio (i.e., the area of the openings divided by the area of the entire façade) is equal to 0.27. Below the façade, an unreinforced masonry shallow foundation with a depth of 600 mm and a thickness of 500 mm was modelled. The façade, lintels and foundation are discretized using a mesh size of 100 mm x 100 mm, with 8-node quadratic plane stress elements with 3 x 3 Gaussian integration schemes. The selected masonry material properties are retrieved from the Dutch Standard (NPR9998:2020en, 2021) and previous studies (Korswagen et al., 2017, Schreppers et al., 2016) and correspond to a baked clay brickwork. An orthotropic, rotating, smeared crack/crush constitutive law (Engineering Masonry Model (Schreppers et al., 2016)) is employed to explicitly simulate the cracking behaviour of masonry.
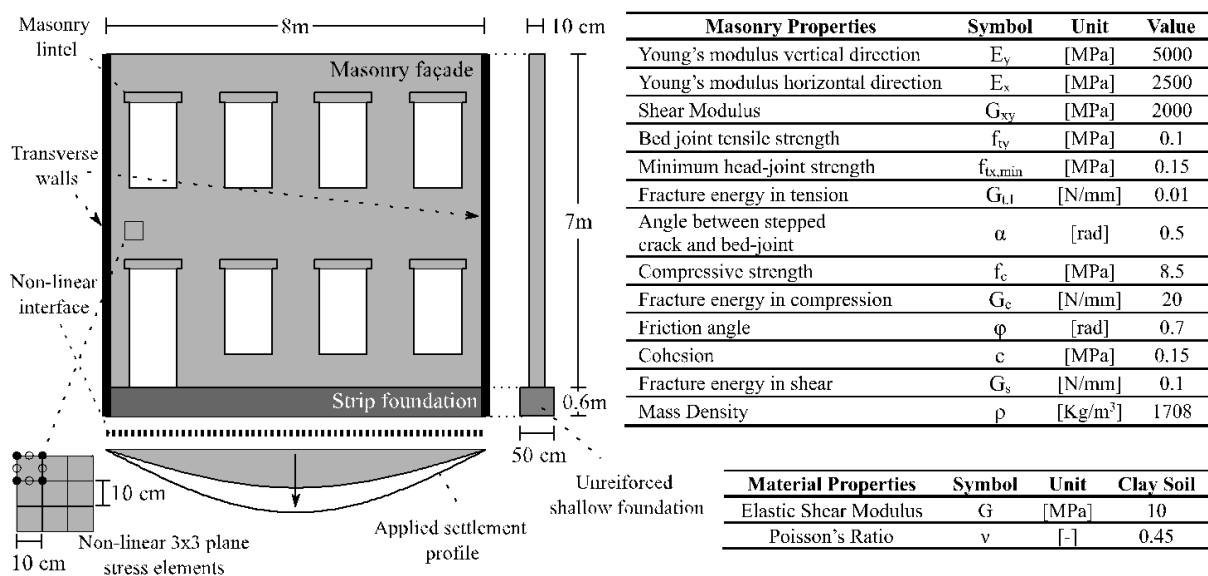

Masonry Properties	Symbol	Unit	Value
Young's modulus vertical direction	E_y	[MPa]	5000
Young's modulus horizontal direction	E_x	[MPa]	2500
Shear Modulus	G_{xy}	[MPa]	2000
Bed joint tensile strength	f_{ty}	[MPa]	0.1
Minimum head-joint strength	$f_{tx,min}$	[MPa]	0.15
Fracture energy in tension	$G_{t,l}$	[N/mm]	0.01
Angle between stepped crack and bed-joint	α	[rad]	0.5
Compressive strength	f_c	[MPa]	8.5
Fracture energy in compression	G_c	[N/mm]	20
Friction angle	φ	[rad]	0.7
Cohesion	c	[MPa]	0.15
Fracture energy in shear	G_s	[N/mm]	0.1
Mass Density	ρ	[Kg/m³]	1708

Material Properties	Symbol	Unit	Clay Soil
Elastic Shear Modulus	G	[MPa]	10
Poisson's Ratio	ν	[-]	0.45

Figure 1. Illustration of the modelled masonry façade and the adopted FE modelling approach.

The constitutive law and the masonry material properties are used for both the façade and foundation, while for the lintels a rotation of 90° of the local axes is considered to model the different orientation of the masonry (soldier brick pattern). Moreover, class-III Mindlin beam elements are placed on the two lateral sides of the façades to simulate the presence of transversal, house-to-house separation walls, which may play an important role when analysing settlement deformations (Korswagen et al., 2019a). As for the soil-structure interaction, a zero-tension interface is modelled by means interface elements, connected to the bottom edge of the foundation. The interface's translational stiffnesses (i.e., Kn and Kt, the vertical and tangential stiffness respectively) are estimated with the equations proposed by (Gazetas, 1991) and et al. (Mylonakis et al., 2006), reported by (NEHRP, 2012), on the basis of soil shear modulus G, Poisson's ratio , and the foundation thickness. The selected soil properties idealize the behaviour of a clayey soil, retrieved from the analysis of the soil stratigraphy in the Groningen region by Arup (ARUP, 2015). The shear modulus G refers to the superficial (i.e. first five meters below the ground surface) soil, in which the strip foundation is assumed to be embedded. Eight settlement configurations (i.e., four hogging and four sagging profiles), computed from using a Gaussian curve (Peck, 1969) described by equation (1), are based on field and literature data (Charles and Skinner, 2004, De Vent, 2011) and idealize the ground displacements due to long-term (i.e. decades) different drivers (e.g., consolidation due to the weight of the structure, organic soil oxidation, soil shrinkage) and are imposed as applied displacements at the base of the foundation (Figure 2).

$$S_{v(x)} = S_{v,max} e^{\left(\frac{-x^2}{2 x_i^2}\right)} \qquad (1)$$

Where $S_{v(x)}$ represents the vertical ground settlement, x_i is the distance from the symmetric axis of the curve to the point of inflection and $S_{v,max}$ is imposed to fix the same distortion for all the profiles. The horizontal ground displacements have been disregarded in this study, since they are not a substantial component for buildings settling under their own weight, as in the adopted numerical model (Boscardin and Cording, 1989). The angular distortion β is used to quantify the intensity of the settlement distortions allowing to compare the results from different settlement shapes. All the computed settlement profiles present up to a maximum ground relative rotation β of 1/10. A sequence of two phases is used in the analysis: first the self-weight of the structure is applied to compute the initial stress-state, and then the settlement profiles are applied. The displacement field due to the self-weight, is cleared before the application of the settlement deformations. While the self-weight is applied using 10 load steps, the number of load steps depended on the magnitude of the maximum settlement of each settlement profile. For each settlement trough, three load rates are considered: i) 0.1 mm/step for a vertical displacement minor or equal to 10 mm, then ii) 0.2 mm/step for a vertical displacement minor or equal to 100 mm and finally iii) 0.5 for higher vertical displacements. Both the gravity and the settlement loads make use of the Quasi-Newton iterative procedure. The tabulated results of the numerical analyses are used to directly quantify the progression of the damage by means of a parameter (Ψ, proposed by (Korswagen et al., 2019b)), based on the number of cracks, their length and opening. The damage severity is then categorised according to the system proposed by (Burland et al., 1978) (Table 1), typically adopted for settlement-related damage.
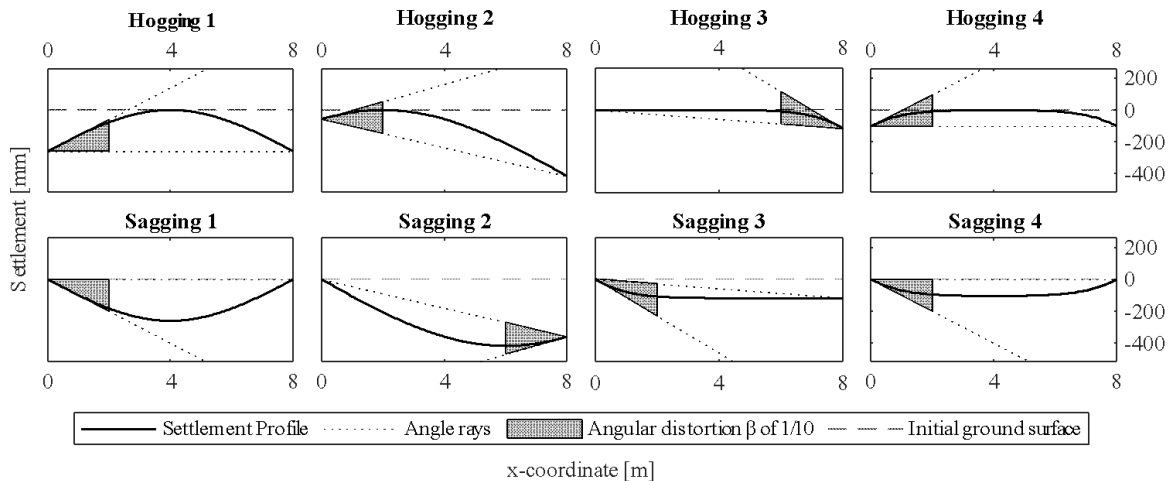
Figure 2. The settlement profiles computed from a Gaussian distribution for a façade of 8 meters. The angular distortion β equal to 1/10, defined accordingly to the definition proposed by Burland and Worth (Burland and Wroth, 1975) and illustrated as a shaded area, was used to generate the different shapes: four hogging (Hogging 1 to 4) and four sagging (Sagging 1 to 4) describe different realist combinations of the vertical displacement, distortion and tilt of the building. The aspect ratio of the axes is set to ensure the preservation of the angles, so that the angular distortion is visually comparable for the different plots.

The settlement parameters (i.e., the differential settlement δρ, the rotation θ and the deflection Δ/L, as originally defined by (Burland and Wroth, 1975) are computed from the vertical displacement at the façade's base (top edge of the foundation) for each step of the analyses, and related to the Ψ damage parameter, allowing a comparison among the performance of the different settlement indicators.

Table 1. Damage scale with classification of visible damage and discretization of the damage parameter in sub-levels (adapted from Burland and Worth (Burland and Wroth, 1975), and Korswagen et al. (Korswagen et al., 2019b)).

Damage level	Degree of damage	Approximate crack width	Parameter of damage
DL0	No Damage	Imperceptible cracks	$\Psi < 1$
DL1	Negligible	up to 0.1 mm	$1 \leq \Psi < 1.5$
DL2	Very slight	up to 1 mm	$1.5 \leq \Psi < 2.5$
DL3	Slight	up to 5 mm	$2.5 \leq \Psi < 3.5$
DL4	Moderate	5 to 15 mm	$\Psi \geq 3.5$

Results of the FE models

The values of settlement indicators against the corresponding damage parameter are reported in Table 2. The assumed settlement shapes highly influence the attainment of a damage level under a given distortion. For instance, for Ψ equal to 1.5, corresponding to multiple cracks with a width of 1 mm, the values or the applied angular distortion varies from about 0.19 ‰ (or 1/5382) to 0.51 ‰ (or 1/1961), a difference factor of 2.7. In the case of Hogging 1 and 2 (Figure 2), the modelled façade exhibits a more vulnerable behaviour, characterized by values of the angular distortion of about two times smaller if compared with the corresponding sagging profiles. The opposite behaviour is observable in the case of Hogging and Sagging 3 and 4, for values of Ψ higher than 1.5. The difference in the behaviour can be explained by the difference in the settlement shapes, since for Hogging 3 and 4 the displacement concentrates in the side(s) of the façade, whereas in the corresponding Sagging profiles the entire façade is settling. Among all the profiles, Hogging 1 is the one associated with the most vulnerable conditions regarding the damage initiation, since the cracking initiates for the smallest value of the angular distortion (i.e., β equals to 0.08 ‰ or 1/13204 for Ψ equal to 0.5 in Table 2).

Table 2. Results of the numerical model in terms of the settlement parameters (i.e., angular distortion, rotation, deflection ratio and differential settlement), computed from the displacements at the façade's base, corresponding to each damage level Ψ. The mean value and the coefficient of variation (CV) are reported for each parameter. For each parameter a colour scheme is applied to distinguish between the lowest (white cells) and the highest (dark grey cells) values.

	Hog.1	Hog.2	Hog.3	Hog.4	Sag.1	Sag.2	Sag.3	Sag.4	Mean	CV
Ψ	Angular distortion β [mm/mm]								
0.5	1/13204	1/12374	1/10250	1/12682	1/6319	1/7792	1/4382	1/5469	1/7762	0.44
1.0	1/8540	1/8141	1/7290	1/8424	1/4440	1/5474	1/2899	1/3825	1/5298	0.44
1.5	1/5382	1/4608	1/4374	1/4759	1/2834	1/3391	1/1961	1/2514	1/3337	0.38
2.0	1/3121	1/2990	1/3163	1/3069	1/2386	1/2806	1/1393	1/2199	1/2465	0.33
2.5	1/2236	1/2236	1/2670	1/2318	1/1613	1/1812	1/1078	1/1567	1/1803	0.32
3.0	1/1887	1/1788	1/2203	1/1808	1/1094	1/1134	1/764	1/1079	1/1306	0.38
3.5	1/1471	1/689	1/1741	1/1390	1/656	1/676	1/475	1/722	1/807	0.43
Ψ	Rotation θ [mm/mm]								
0.5	1/13052	1/3016	1/3848	1/12449	1/6268	1/1359	1/1962	1/5390	1/3420	0.78
1.0	1/8386	1/2217	1/2633	1/8214	1/4401	1/974	1/1310	1/3768	1/2385	0.77
1.5	1/5207	1/1543	1/1662	1/4563	1/2799	1/600	1/874	1/2469	1/1528	0.78
2.0	1/3006	1/804	1/1059	1/2971	1/2358	1/563	1/601	1/2152	1/1113	0.67
2.5	1/2089	1/699	1/864	1/2178	1/1589	1/378	1/475	1/1530	1/837	0.68
3.0	1/1729	1/560	1/775	1/1648	1/1071	1/256	1/359	1/1048	1/623	0.74
3.5	1/1363	1/281	1/683	1/1269	1/644	1/206	1/271	1/690	1/442	0.68
Ψ	Deflection ratio Δ/L [mm/mm]								
0.5	1/47206	1/44864	1/46668	1/52128	1/22597	1/21677	1/24306	1/22407	1/30741	0.38
1.0	1/30805	1/31685	1/31456	1/34735	1/15885	1/15264	1/15971	1/15654	1/21077	0.37
1.5	1/19918	1/20103	1/19348	1/19749	1/10687	1/10251	1/10675	1/10235	1/13681	0.33
2.0	1/11203	1/11250	1/10553	1/11687	1/8270	1/7989	1/7648	1/7920	1/9285	0.18
2.5	1/8279	1/8607	1/7845	1/8798	1/5384	1/5099	1/5388	1/5310	1/6484	0.24
3.0	1/6877	1/6499	1/6385	1/6751	1/3758	1/3626	1/3923	1/3606	1/4767	0.30
3.5	1/4814	1/1741	1/4949	1/4585	1/2466	1/2270	1/2589	1/2263	1/2781	0.38
Ψ	Differential settlement δρ [mm]								
0.5	0.17	2.22	1.30	0.16	0.36	4.84	2.25	0.37	1.46	1.11
1.0	0.27	2.99	1.94	0.24	0.51	6.72	3.35	0.53	2.07	1.09
1.5	0.43	4.20	2.99	0.44	0.77	10.97	5.08	0.81	3.21	1.13
2.0	0.76	8.02	5.02	0.72	0.99	11.30	7.56	1.05	4.43	0.94
2.5	1.08	9.06	6.19	1.01	1.52	16.67	9.41	1.56	5.81	0.97
3.0	1.34	11.38	6.51	1.37	2.20	23.89	11.14	2.31	7.52	1.04
3.5	1.86	16.53	6.91	1.99	3.34	24.39	11.50	3.73	8.78	0.93

The performance of the different settlement indicators is compared by means of the coefficient of

variation (CV) for all the Ψ values. Although all the settlement parameters have similar values of the CV, the best indicator is the deflection ratio Δ/L, with the lowest values (ranging from 0.18 to 0.38), followed by the relative rotation β (from 0.32 to 0.44), the rotation θ (from 0.67 to 0.78) and the differential settlement δρ (with values ranging from 0.94 to 1.11).

Discussion and conclusions

This paper demonstrates the use of finite element models to investigate the response of masonry structures subjected to ground settlements. Due to the unpredictability of the subsidence-related settlements not only in terms of magnitude but also of shape, eight settlement profiles idealize the vertical ground displacements on the base of field observations and literature data. The horizontal ground displacements are purposely neglected. The severity of the damage is objectively and directly quantified by means of the proxy parameter for damage Ψ. Then, the selected settlement indicators (i.e., angular distortion, rotation, deflection ratio and differential settlement) are related to the progression of the damage to investigate their dependency on the settlement shape. Among the settlement indicators, the lowest variability is observed for the deflection ratio, although they all vary significantly depending on the settlement shape. Such variability provides a warning for the use of deterministic limiting values, due to the unpredictively of the shape of ground deformations. For instance, to avoid the occurrence of a serviceability limit state, the Dutch standard (NEN9997-1+C2:2017nl, 2017) proposes values of angular distortion ranging from 2.00 ‰ (or 1/500, as suggested in the Eurocode 7 (CEN, 2004)) up to 5.00 ‰ (or 1/200) for sagging settlement profiles; these values are halved for hogging profiles. In this study, the difference between the angular distortion in hogging and sagging is indeed ranging from 1.1 up to 2.6. The serviceability limit state has been associated in previous studies with the occurrence of cracks above 5 mm wide (Ψ higher or equal to 3.5 in this study) (Rankin, 1988, Yunusa et al., 2013). For Ψ equal to 3.5, the corresponding values of the angular distortion range from 1.24 ‰ (or 1/807) up to 2.11 ‰ (or 1/475) for sagging and from 0.57 ‰ (or 1/1741) up to 1.45 ‰ (or 1/689) for hogging, depending on the settlement shape. Thus, the thresholds proposed in the guideline are higher than the values observed in this study of a factor of 1.1 up to 2.5. The results of the numerical model are thus conservative estimates of the façade response, since settlements developing over long times may allow the structure to accommodate the deformations with limited or without any damage. Nevertheless, this numerical approach can be used to perform additional analyses, considering not only the variability of the settlement profiles, but also different structural features, based on multi-source datasets. Such analyses, in conjunction with engineering judgment, may allow engineers, scientists and local authorities to propose probabilistic limiting values for the ground and/or building's deformations.

Acknowledgments

References

ARUP (2015). *Groningen Earthquakes Structural Upgrading - Site Response Analysis* (229746_032.0_REP141.
Boscardin, M. D. and Cording, E. J. (1989) 'Building Response to Excavation-Induced Settlement', *Journal of Geotechnical Engineering-Asce,* 115(1), pp. 1-21. doi: Doi 10.1061/(Asce)0733-9410(1989)115:1(1)

Burland, J. B., Broms, B. B. and De Mello, V. F. (1978). 'Behaviour of foundations and structures'. doi:

Burland, J. B. and Wroth, C. (1975) *Settlement of buildings and associated damage*.

CEN (2004) *Eurocode 7 Geotechnical design - Part 1: General rules. Final Draft, EN 1997-1:2004 (E), (F) and (G)*.

Charles, J. A. and Skinner, H. D. (2004). 'Settlement and tilt of low-rise buildings', *Proceedings of the Institution of Civil Engineers-Geotechnical Engineering,* 157(2), pp. 65-75. doi. Available at: <u><Go to ISI>://WOS:000222166400003</u>

De Vent, I. A. E. (2011). 'Structural damage in masonry: Developing diagnostic decision support'. doi:

Drougkas, A., Verstrynge, E., Van Balen, K., Shimoni, M., Croonenborghs, T., Hayen, R. and Declercq, P. Y. (2020) 'Country-scale InSAR monitoring for settlement and uplift damage calculation in architectural heritage structures', *Structural Health Monitoring-an International Journal*, pp. 1475921720942120. doi: Artn 1475921720942120 10.1177/1475921720942120

Gazetas, G. (1991). 'Foundation vibrations', *Foundation engineering handbook*: Springer, pp. 553-593.

Korswagen, P., Longo, M., Meulman, E. and Van Hoogdalem, C. (2017) 'Damage sensitivity of Groningen masonry structures–experimental and computational studies', *Delft University of Technology. Report,* (C31B69WP0-12).

Korswagen, P. A., Longo, M., Meulman, E. and Rots, J. 'Experimental and computational study of the influence of pre-damage patterns in unreinforced masonry crack propagation due to induced, repeated earthquakes'. *13th North American Masonry Conference*: TMS, 1628-1645.

Korswagen, P. A., Longo, M., Meulman, E. and Rots, J. G. (2019b). 'Crack initiation and propagation in unreinforced masonry specimens subjected to repeated in-plane loading during light damage', *Bulletin of Earthquake Engineering,* 17(8), pp. 4651-4687.

Mylonakis, G., Nikolaou, S. and Gazetas, G. (2006). 'Footings under seismic loading: Analysis and design issues with emphasis on bridge foundations', *Soil Dynamics and Earthquake Engineering,* 26(9), pp. 824-853. doi: 10.1016/j.soildyn.2005.12.005

NEHRP (2012). *NIST GCR 12-917-21 Soil–structure interaction for building structures*, Gaithersburg: National Institute of Standards and Technology, US Department of Commerce.

NEN9997-1+C2:2017nl (2017). 'Geotechnisch ontwerp van constructies - Deel 1: Algemene regels (*Geotechnical design of structures - Part 1: General rules*)'.

NEN (2021). *Assessment of structural safety of buildings in case of erection, reconstruction and disapproval - Induced earthquakes - Basis of design, actions and resistances*.

Peck, R. B. (1969). 'Deep excavations and tunneling in soft ground', *Proc. 7th ICSMFE, 1969*, pp. 225-290.

Rankin, W. (1988). 'Ground movements resulting from urban tunnelling: predictions and effects', *Geological Society, London, Engineering Geology Special Publications,* 5(1), pp. 79-92.

Schreppers, G., Garofano, A., Messali, F. and Rots, J. (2016). 'DIANA validation report for masonry modelling', *DIANA FEA report*.

Yunusa, G. H., Hamza, U., Abdulfatah, A. Y. and Suleiman, A. (2013). 'Geotechnical investigation into the causes of cracks in building: A case study', *Electronic Journal of Geotechnical Engineering,* 18, pp. 2823-2833.